THE JOURNAL OF PHYSICAL CHEMISTRY B
A JOURNAL OF THE AMERICAN CHEMICAL SOCIETY

pubs.acs.org/JPCB

Article

Synthesis, Optical Spectroscopy, and Laser and Biomedical Imaging Application Potential of 2,4,6-Triphenylpyrylium Tetrachloroferrate and Its Derivatives

Pradip K. Bhowmik,* David King, Si L. Chen, Ronald Carlo G. Principe, Haesook Han, Egor Evlyukhin, Petrika Cifligu, Ahamed Jubair, Vladimir Kartazaev, Swapan K. Gayen, Shane T. Killarney, Julia D. Caci, and Kris C. Wood

Cite This: *J. Phys. Chem. B* 2024, 128, 9815−9828

Read Online

ACCESS | Metrics & More | Article Recommendations | Supporting Information

ABSTRACT: Synthesis, optical spectroscopic properties, two-photon (TP) absorption-induced fluorescence, and laser and bioimaging application potentials of 2,4,6-triphenylpyrylium tetrachloroferrate (**1**),4-(4-methoxyphenyl)-2,6-diphenylpyrylium tetrachloroferrate (**2**), 2,6-bis(4-methoxyphenyl)-4-phenylpyrylium tetrachloroferrate (**3**), and 2,4,6-tris(4-methoxyphenyl)pyrylium tetrachloroferrate (**4**) are presented. The synthesis involves the conversion of pyrylium tosylates to pyrylium chlorides, followed by transformation into **1**−**4** on heating to reflux with $FeCl_3$ in acetonitrile. They are characterized using ^1H and ^{13}C NMR spectra in CD_3OD, and FTIR and Raman spectroscopic techniques. The salts dissolve in organic solvents and water (pH = 7 to 3) even at high concentrations (10^{-3} M). These solutions absorb light strongly from 500−300 nm. Solutions of **1**, **3**, and **4** fluoresce with high quantum yield in the 500−700 nm spectral range. Salts **1** and **4** exhibit fluorescence lifetime shortening, line width narrowing, and free-running laser action under intense pulsed laser excitation. Toxicity and cell imaging studies using human cancer cell lines reveal that salts **1** and **3** function as cellular fluorophores *in vitro* and have no adverse effects on cellular viability at nanomolar ranges. Furthermore, acetonitrile and methanol solutions of salts **1**, **3**, and **4** exhibit strong two-photon absorption-induced fluorescence, opening potential applications in biomedical imaging and microscopy.

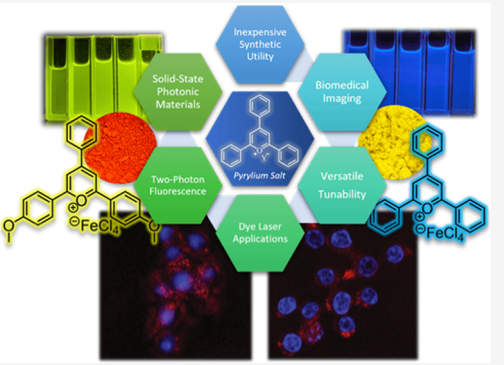

1. INTRODUCTION

Organic molecules with favorable optical spectroscopic properties are finding increasing applications in photonic and optoelectronic devices, such as organic photovoltaics (PVs) and organic light-emitting diodes (OLEDs) and paving the way for the development of organic electronics. Salient features of photoactive organic molecules include potential for lower-cost, green synthesis and processing, as well as simpler and nimbler manufacturing compared to their inorganic counterparts.[1,2] This article reports on the synthesis, optical spectroscopic properties, and laser and bioimaging potentials of a group of organic molecules 2,4,6-triphenylpyrylium tetrachloroferrate and its derivatives.

Pyrylium (Py) salts represent a class of small organic molecules built on a six-membered cationic heterocyclic structure with one positively charged oxygen ion and a variety of counterions, such as Cl^-, ClO_4^-, BF_4^-, PF_6^-, TsO^-, Tf_2N^-, and $FeCl_4^-$.[3] For more than a century, these salts have had versatile applications ranging from synthetic utility for the construction of heterocyclic compounds, complex macrocycles, or metallo-supramolecules to photosensitizers in organic transformations to radical and cationic photopolymerization reactions, and even to metal-free ring-opening metathesis polymerization reactions.[3−7] Favorable optical absorption and fluorescence properties of Py-salts have been exploited to design chemosensors and biosensors for cyanide ions,[8] nitric oxide,[9] amines, amino acids, and proteins.[10]

Dyes dissolved in common solvents have been used as active materials for wavelength tunable lasers, fluorescent markers, and saturable absorbers and in numerous other linear and nonlinear optical (NLO) applications since the early days of lasers. More recently, dye-based novel structures, such as metamaterials, surface-supported nanofilms, self-assembled nanostructures, thin polymeric films, and dye-dispersed solid matrices have been explored for different light emission, NLO, and photonic device potentials.[11−16] However, the light emission, lasing potential, NLO properties, and feasibility for

Received: June 13, 2024
Revised: September 10, 2024
Accepted: September 17, 2024
Published: September 27, 2024

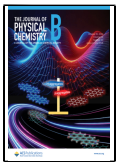

https://doi.org/10.1021/acs.jpcb.4c03934
J. Phys. Chem. B 2024, 128, 9815−9828

use as contrast agents for biomedical imaging applications of these salts have received limited or little attention. Schäfer et al.[17] first explored the performance of several Py-salts as laser dyes by exciting them with 2.5 ns, 337 nm light pulses from a nitrogen laser. However, they did not specify the efficiency and tunability of the laser operation. In an extended study, Tripathi et al.[18] observed "laser effects" in a series of rigidized (wherein the free rotation of the single bond of the phenyl group to the pyrylium ring is restricted), various substituted pyrylium and thiopyrylium salts with ClO_4^- counterions dissolved in organic solvents and compared their performance with that of Rhodamine6G (R-6G) solution, a highly efficient laser dye. Using acetonitrile (CH_3CN) and dichloromethane (CH_2Cl_2) as solvents and pumping with 337 nm, 8 ns, 5 Hz repetition-rate pulses from a nitrogen laser, they demonstrated tunable laser operation over the 505−655 nm range. No lasing properties were observed in ethanol solutions of these Py-salts.[12] Kotowski et al.[19] carried out a similar study involving 34 rigidized pyrylium and 2 thiopyrylium salts with ClO_4^- counterions dissolved in acetonitrile, methanol, and other chlorinated solvents and compared their performance with those of R-6G and Coumarin-102. Twenty of these salts lased with an efficiency better than 10%, and a few had wavelength tunability of ∼80 nm. On the other hand, several nonrigidized (wherein the free rotation of the single bond of phenyl group to the pyrylium ring is not restricted) Py-salts with BF_4^- counterions show laser action in acetone.[20] The 2,4,6-triphenylpyrylium salt with tosylate counterions, 2,4,6-tris(4-chlorophenyl)pyrylium with Tf_2N^- counterions and 2,4,6-tris(4-methoxyphenyl)pyrylium with Tf_2N^- counterions lase in acetonitrile.[21,22] Interestingly enough, even 2,4,6-triphenylpyrylium chloride shows laser action in dichloromethane (DCM), methanol, ethanol, and acetonitrile but not in acidic aqueous solution.[23] Thus, it appears that the lasing criteria for diverse rigidized and nonrigidized Py-salts in different organic solvents with regard to their chemical structures need further exploration. Since the Py-salts are cationic, there exists a choice of variation of anionic counterions that will enable one to dissolve Py-salts in organic solvents, even in water, at high (∼10^{-3} M) concentrations necessary for a dye laser operation.

In general, Py-salts for dye laser applications must have sufficient solubility and stability in target solvents and high fluorescence quantum yields. It is reported that the lasing properties of Py-salts are independent of the counterions that are limited to include ClO_4^-, BF_4^-, and Br^-.[12] It is also reported that these salts with different anions will have different solubility in organic solvents and water depending on the anion structures.[24] Lasing properties of these salts in various solvents, especially benign solvents, including water, are of considerable interest.

The solubility of Py-salts in water has been studied as early as 1984 by Katritzky et al.[25−27] by the introduction of three sulfonic or carboxylic groups attached to the phenyl groups as solubilizing groups. These Py-salts with ClO_4^- as counterions are water-soluble. In aqueous solutions, all salts are in equilibrium with the corresponding enedione pseudobases and their anions, and the concentrations of the respective anions of pseudobases depend on the pH of the solutions.[25−27] It is reported[28] that Py-salts with organic counterions as solubilizing anions such as hydroxybenzenesulfonate and $(HOCH_2)_3CNHCH_2CH_2SO_3^-$ are soluble in water, but to our knowledge, their fluorescence properties have not yet been reported. Ye et al.[29] communicated that the Py-salts (**1**−**4**) with $FeCl_4^-$ (inorganic counterion) are water-soluble. They reported the fluorescence properties of these salts in DCM (1×10^{-5} M) and water (1×10^{-5} M). However, the question of whether these salts are stable in an acidic aqueous solution or pure water and the extent of their solubility in water was not addressed. It is well-known that these salts undergo hydrolytic ring opening to form their pseudobases in water at neutral pH. The ring-opening reaction rate depends on the pH of the medium: the lower the pH, the slower the ring-opening reaction. This process is inhibited for pH values of 3 or lower.[30] The stability of Py-salts against ring opening in water (pH = 3−7) is a challenging task that needs to be addressed for the exploitation of their optical spectroscopic properties in aqueous solutions.

There are even fewer reports on the NLO properties of pyrylium salts. Fakis et al.[20] reported strong TPA-induced fluorescence (TPAIF) in three BF_4^- substituted Py-salts.[20] The same group then studied intensity-dependent nonlinear absorption in five Cl-substituted pyrylium chromophores using near-infrared femtosecond pulsed excitation to assess their potential applications as optical limiters.[31] The group further investigated the TPAIF in several $-OCH_3$, $-CH_3$, −H, and −Cl-substituted Py-salts and explored their potential in three-dimensional data storage in polymer matrices.[32] In addition, these TPA properties of Py-salts are theoretically predicted.[33] In recent years, TPA properties are gaining considerable interest because they find a wide range of potential applications including upconverted lasing, optical power limiting, two-photon laser microscopy, photodynamic therapy, microfabrication, and optical data storage.[31−33]

In this article, we focus on four Py-salts with $FeCl_4^-$ counterions: 2,4,6-triphenylpyrylium tetrachloroferrate (**1**), 2,6-phenyl-4-(4-methoxyphenyl)pyrylium tetrachloroferrate (**2**), 2,6-bis(4-methoxyphenyl)-4-phenylpyrylium tetrachloroferrate (**3**), and 2,4,6-tris(4-methoxyphenyl)pyrylium tetrachloroferrate (**4**). Our interest in these salts derives from their (a) high solubility in common organic solvents, such as acetonitrile, methanol, ethanol, etc., (some are even highly soluble in water); (b) high fluorescence quantum yield of those solutions compared to Py-salts with other substituents such as −H, $-CH_3$, −F, −Cl, −Br,[12−14] and (c) substantial TPA-induced fluorescence. Solubility in high concentration (∼10^{-3} M) and high fluorescence quantum yields are essential for application as active materials for dye laser application. Solubility in safe organic solvents (water, in particular) and strong fluorescence are highly desirable for fluorescence-based biomedical imaging, photodynamic therapy, and other "green chemistry" and eco-friendly applications. Strong TPAIF and high quantum yields are crucial for high-resolution two-photon fluorescence imaging of deep tissues using near-infrared excitation.

2. METHODS

2.1. Materials. The chemicals and spectral-grade solvents were procured from commercial suppliers MilliporeSigma and TCI America, and used without further purification. The ^1H and ^{13}C NMR spectra were recorded using a Varian NMR 400 MHz spectrometer equipped with two radiofrequency (RF) channels at room temperature. The NMR sample solutions were prepared by dissolving 10 mg of the compound in d_6-DMSO or $CDCl_3$ with tetramethylsilane as an internal standard. Fourier transform infrared (FTIR) spectra were recorded by using a Shimadzu spectrometer (IR Affinity-1)

https://doi.org/10.1021/acs.jpcb.4c03934
J. Phys. Chem. B 2024, 128, 9815−9828

Scheme 1. Multistep synthesis of 1−4 from acetophenones and benzaldehydes

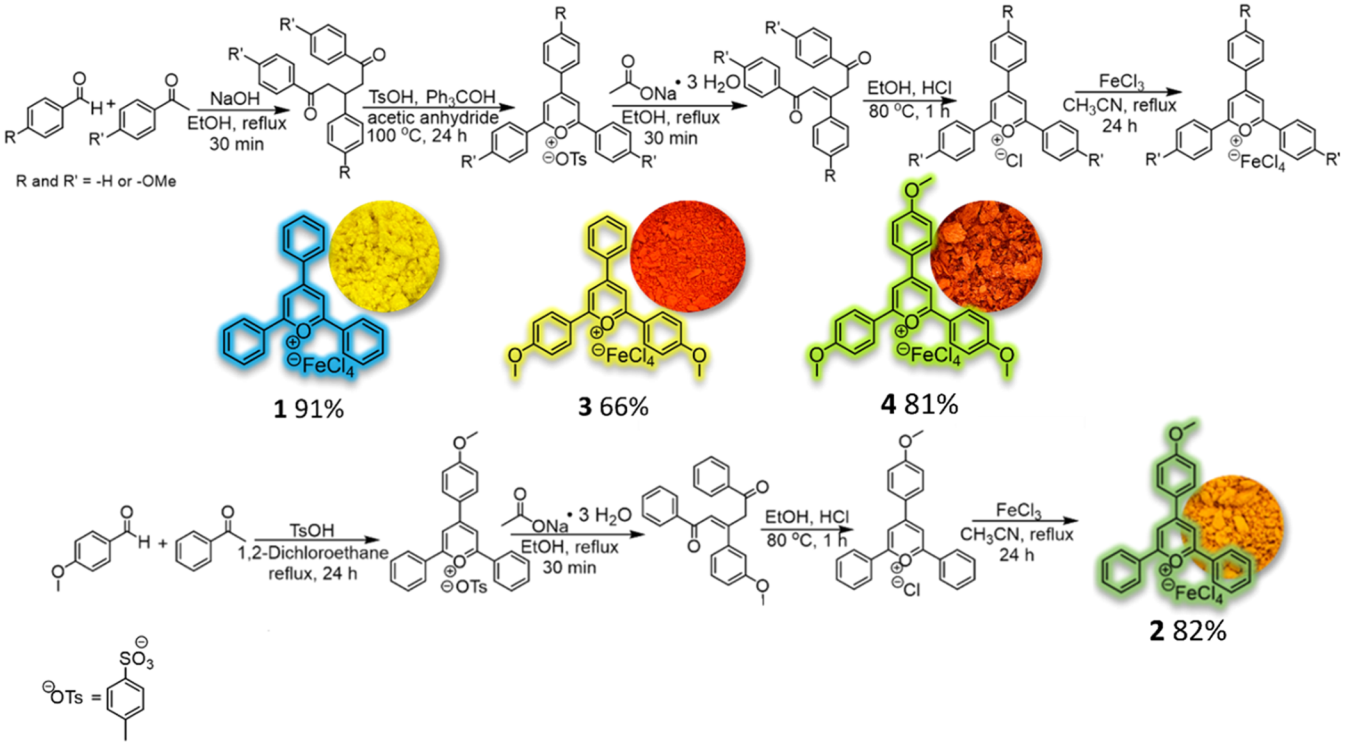

with KBr pellets. Elemental analyses of the salts were obtained from the Atlantic Microlab Inc., Norcross, GA. Raman spectroscopy was conducted at GSECARS (Sector 13) at the Advanced Photon Source. An excitation wavelength of 660 nm was used and detailed information about the experimental setup is reported elsewhere.[34]

2.2. Synthesis of 2,4,6-Triphenylpyrylium Tetrachloroferrate and Its Derivatives 1−4. Pyrylium tosylate was prepared by a two-step procedure via the 1,5-diketone according to the procedure described in the literature.[21,22] Data for 2,4,6-triphenylpyrylium tosylate: mp = 222 °C (peak maximum by DSC).[21] IR (cm^{-1}): 3066, 2914, 1624, 1500, 1448, 1199, 1122, 1033, 767. ^{1}H NMR (DMSO-d_6, 400 MHz) δ 9.18 (2H, s), 8.61 (6H, d, J = 7.2 Hz), 7.89 (3H, t, J = 7.6 Hz), 7.80−7.77 (6H, m), 7.48 (2H, d, J = 6.4 Hz), 7.11 (2H, d, J = 8.0 Hz), 2.28 (s, 3H). ^{13}C NMR (DMSO-d_6, 100 MHz) δ: 170.5, 165.5, 146.3, 137.9, 135.6, 135.4, 132.9, 130.5, 130.3, 130.2, 129.5, 129.2, 128.4, 125.9, 115.6, 21.2. Anal. Calculated (found) for $C_{30}H_{24}O_4S$: C, 74.98 (74.87); H, 5.03 (5.16); S, 6.67 (6.54).

Data for 4-(4-methoxyphenyl)-2,6-diphenylpyrylium tosylate: mp = 200−202 °C. ^{1}H NMR (CD_3OD, 400 MHz) δ 8.82 (2H, s), 8.51 (2H, d, J = 9.2 Hz), 8.44 (4H, d, J = 7.2 Hz), 7.82−7.67 (8H, m), 7.25−7.17 (4H, m), 3.98 (3H, s), 2.34 (s, 3H). ^{13}C NMR (CD_3OD, 100 MHz) δ: 167.68, 166.69, 164.68, 142.28, 140.13, 134.50, 132.46, 129.71, 129.30, 128.34, 128.04, 125.54, 124.57, 115.58, 115.82, 55.34, 19.88.

Data for 2,6-bis(4-methoxyphenyl)-4-phenylpyrylium tosylate: mp = 218 °C, (peak maximum by DSC).[21] IR (cm^{-1}): 3061, 2937, 1622, 1602, 1491, 1263, 1120, 1031, 773. ^{1}H NMR (DMSO-d_6, 400 MHz) δ 8.88 (2H, s), 8.55 (6H, m), 7.82 (1H, t, J = 7.2 Hz), 7.76 (2H, t, J = 7.2 Hz), 7.49 (2H, d, J = 8.0 Hz), 7.31 (4H, d, J = 9.2 Hz), 7.11 (2H, d, J = 8.0 Hz), 3.97 (6H, s), 2.28 (3H, s). ^{13}C NMR (DMSO-d_6, 100 MHz) δ: 169.3, 165.2, 163.6, 146.2, 137.9, 134.9, 133.1, 131.4, 130.1, 130.0, 128.4, 125.9, 121.8, 115.8, 113.1, 56.5, 21.2. Anal. Calculated (found) for $C_{32}H_{28}O_6S$: C, 71.09 (70.52); H, 5.22 (5.25); S, 5.93 (5.79).

Data for 2,4,6-tris(4-methoxyphenyl)pyrylium tosylate: mp = 206 °C, (peak maximum by DSC as monohydrate).[22] ^{1}H NMR (400 MHz, $CDCl_3$) δ ppm 8.45 (d, J = 8.0 Hz, 2H), 8.41 (s, 2H), 8.18 (d, J = 9.2 Hz, 4H), 8.00 (d, J = 8.0 Hz, 2H), 7.22 (d, J = 7.6 Hz, 2H), 6.80 (d, J = 8.8 Hz, 4H), 6.61 (d, J = 9.2 Hz, 2H), 3.76 (s, 6H), 3.60 (s, 3H), 2.39 (s, 3H). ^{13}C NMR (100 MHz, $CDCl_3$) δ ppm: 166.9, 165.2, 164.5, 161.6, 144.9, 138.8, 133.3, 130.5, 128.5, 126.4, 123.9, 120.8, 115.3, 115.2, 110.4, 55.6, 55.4, 21.3. Anal. Calculated (found) for $C_{33}H_{32}O_8S$ (588.68): C, 67.33 (67.93); H, 5.48 (5.32); S, 5.45 (5.45).

It was converted to the pseudobase with the treatment of sodium acetate in ethanol on heating for 30 min according to the reported procedure.[23,35]

Data for 1,3,5-triphenyl-2-pentene-1,5-dione: ^{1}H NMR ($CDCl_3$, 400 MHz, ppm) δ = 8.08 (2H, d, J = 8.0 Hz), 7.99 (2H, d, J = 8.0 Hz), 7.56−7.39 (12H, m), 4.87 (2H, s). ^{13}C NMR ($CDCl_3$, 100 MHz, ppm): δ = 196.1, 190.8, 152.7, 142.0, 139.0, 137.0, 133.1, 132.7, 129.3, 128.7, 128.6, 128.5, 128.3, 126.8, 42.9.

Data for 3-(4-methoxyphenyl)-1,5-diphenyl-2-pentene-1,5-dione: ^{1}H NMR ($CDCl_3$, 400 MHz, ppm) δ = 8.09 (2H, d, J = 7.2 Hz), 7.98 (2H, d, J = 7.2 Hz), 7.60−7.44 (9H, m), 6.93 (2H, d, J = 9.2 Hz), 4.88 (2H, s), 3.83 (3H, s). ^{13}C NMR ($CDCl_3$, 100 MHz, ppm): δ = 196.31, 190.74, 160.78, 152.40, 139.37, 137.06, 134.07, 133.06, 132.51, 128.61, 128.51, 128.31, 128.28, 128.22, 121.74, 114.17, 55.39, 42.73.

Data for 1,5-bis(4-methoxyphenyl)-3-phenyl-2-pentene-1,5-dione: ^{1}H NMR ($CDCl_3$, 400 MHz, ppm): δ = 8.05−7.98 (4H, m), 7.54−7.52 (2H, m), 7.41−7.37 (4H, m), 6.96−6.92 (4H, m), 4.82 (2H, s), 3.87−3.86 (6H, m). ^{13}C NMR ($CDCl_3$, 100 MHz, ppm): δ = 194.81, 189.47, 163.47, 163.26, 151.94,

https://doi.org/10.1021/acs.jpcb.4c03934
J. Phys. Chem. B 2024, 128, 9815−9828

142.19, 132.06, 130.64, 130.57, 130.12, 129.07, 128.67, 126.78, 123.73, 113.73, 55.47, 42.44.

Data for 1,3,5-tris(4-methoxyphenyl)-2-pentene-1,5-dione: ^{1}H NMR ($CDCl_3$, 400 MHz, ppm) δ = 8.06−7.97 (4H, m), 7.51−7.49 (2H, d, J = 8.8 Hz), 7.39 (1H, s), 6.96−6.90 (6H, m), 4.83 (2H, s), 3.87−3.86 (6H, m), 3.82 (3H, s). ^{13}C NMR ($CDCl_3$, 100 MHz, ppm): δ = 195.04, 189.40, 163.44, 163.13, 160.56, 151.66, 134.30, 132.33, 130.59, 130.54, 130.16, 128.23, 121.84, 114.08, 113.72, 113.68, 55.47, 55.45, 55.36, 42.25.

The pseudobase was then converted to the chloride salt with the treatment of concentrated HCl/ethanol on heating for 1 h, according to the literature procedure.[23,35]

Data for 2,4,6-triphenylpyrylium chloride: mp 117−120 °C.[35] ^{1}H NMR (CD_3OD, 400 MHz, ppm) δ = 9.00 (2H, s), 8.53 (6H, d, J = 7.6 Hz), 8.45 (3H, t, J = 7.6 Hz), 7.88−7.75 (6H, m). ^{13}C NMR (CD_3OD, 100 MHz, ppm): δ = 171.1, 166.6, 135.0, 134.9, 133.0, 129.9, 129.8, 129.4, 129.2, 128.4, 115.0. Anal. Calculated (found) for $C_{23}H_{17}OCl{\cdot}0.65H_2O$ (356.55): C, 77.48 (77.23); H, 5.17 (4.99).

Data for 4-(4-methoxyphenyl)-2,6-diphenylpyrylium chloride: mp = 195 °C (decom.). ^{1}H NMR (CD_3OD, 400 MHz, ppm) δ = 8.85 (2H, s), 8.53 (2H, d, J = 9.2 Hz), 8.47 (4H, d, J = 7.2 Hz), 7.84−7.74 (6H, m), 7.28 (2H, d, J = 9.2 Hz), 3.99 (3H, s). ^{13}C NMR (CD_3OD, 100 MHz, ppm): δ = 169.70, 166.71, 134.45, 132.45, 129.72, 129.28, 128.25, 128.02, 124.55, 115.58, 112.80, 55.32. Anal. Calculated (found) for $C_{24}H_{19}O_2Cl{\cdot}0.67H_2O$ (386.92): C, 71.73 (71.23); H, 5.52 (5.48).

Data for 2,6-bis(4-methoxyphenyl)-4-phenylpyrylium chloride: mp = 197 °C (decom.). ^{1}H NMR (CD_3OD, 400 MHz, ppm) δ = 8.59 (2H, s), 8.40 (4H, d, J = 8.8 Hz), 8.31 (2H, d, J = 7.2 Hz), 7.80−7.68 (3H, m), 7.24 (4H, d, J = 8.8 Hz), 3.96 (6H, s). ^{13}C NMR (CD_3OD, 100 MHz, ppm): δ = 169.59, 165.71, 164.25, 134.24, 133.12, 130.56, 129.67, 128.90, 121.10, 115.41, 112.15, 55.20.

Data for 2,4,6-tris(4-methoxyphenyl)pyrylium chloride: mp = 200 °C (decom.). ^{1}H NMR (CD_3OD, 400 MHz, ppm): δ = 8.46 (2H, s), 8.36−8.30 (6H, m), 7.20 (6H, m), 3.97−3.95 (9H, m). ^{13}C NMR (CD_3OD, 100 MHz, ppm): δ = 168.50, 165.94, 165.33, 162.63, 131.66, 130.13, 124.63, 121.19, 115.31, 115.26, 110.20, 55.16, 55.10.

Finally, the chloride salt was converted to **1** on heating to reflux in acetonitrile with $FeCl_3$ instead of neat conditions used in the reported procedure.[36] The procedure was as follows: ferric chloride (395 mg, 1.147 mmol) and 2,4,6-triphenylpyrylium chloride (186 mg, 1.147 mmol) were dissolved in 25 mL of acetonitrile and heated to reflux for 24 h. The solvent was removed under reduced pressure and the resulting yellow solid was washed with ether to furnish 530 mg of **1**. mp: 220−225 °C (the ^{1}H and ^{13}C spectra of 4-methoxyphenyl-2,6-diphenylpyrylium salt are given in Figure S1 and those of pseudobases are given in Figures S2−S4). Similarly, **2**−**4** were prepared in accordance with the identical protocols as shown in Scheme 1. The presence of $FeCl_4^-$ in **1**−**4** precluded the characterization of these salts from the analyses of their ^{1}H and ^{13}C NMR spectra, but their precursor chloride salts were characterized from the analyses of their ^{1}H and ^{13}C NMR spectra (Figures S5−S7). These NMR spectra clearly characterize that the cation moieties of **1**−**4** are pyrylium cations. The pyrylium moieties were characterized from the analyses of their IR spectra (Figures S8−S11) and $FeCl_4^-$ ions were characterized by the presence of a Fe−Cl band at 332, 335, 321, and 321 cm^{-1} from the analyses of Raman spectra (Figures S12−S15) for these salts.[29] The purity of **1**−**4** was also determined from their elemental analyses.

Data for **1** are mp = 250−252 °C. IR (KBr, ν cm^{-1}): 1616, 1592, 1497, 1259. Anal. Calculated (found) for $C_{23}H_{17}Cl_{14}FeO$ (507.09): C, 54.48 (54.21); H, 3.38 (3.44).

Data for **2** are mp = 230−233 °C. IR (KBr, ν cm^{-1}): 1633, 1583, 1486, 1243, 1180. Anal. Calculated (found) for $C_{24}H_{19}Cl_{14}FeO_2$ (537.06): C, 53.67 (53.70); H, 3.57 (3.48).

Data for **3** are mp = 220−226 °C. IR (KBr, ν cm^{-1}): 1616, 1601, 1484, 1257, 1172. Anal. Calculated (found) for $C_{25}H_{21}Cl_{14}FeO_3$ (567.09): C, 52.95 (53.16); H, 3.73 (3.70).

Data for **4** mp = 260−262 °C (decom.). IR (KBr, ν cm^{-1}): 1628, 1583, 1511, 1458, 1261, 1174. Anal. Calculated (found) for $C_{26}H_{23}Cl_{14}FeO_4$ (597.11): C, 52.30 (52.47); H, 3.88 (3.85).

2.3. Optical Spectroscopic Measurements. The room temperature fluorescence spectra, excitation spectra, and quantum yields of **1**−**4** solutions were measured using the pertinent mode of operation of a PerkinElmer FL 6500 luminescence spectrometer. Fluorescence lifetime and fluorescence spectra of the salt solutions as a function of excitation intensity were measured using a femtosecond Ti: sapphire laser system (Spectra-Physics Spitfire) and a Streak Camera (SC) system (Hamamatsu Streak Scope C4334) coupled with a spectrometer (Imaging Spectrograph G50is). The laser oscillator system generated 800 nm, 130 fs duration, 82 MHz repetition rate pulses. A pulse picker and a regenerative amplifier provided amplified pulses at 1 kHz repetition rate. The second harmonic of these pulses at 400 nm was used for linear (one-photon) excitation of each salt solution contained in a quartz cuvette, while the 800 nm beam was used for two-photon excitation experiments. An optical fiber connected with the SC spectrometer collected a fraction of the fluorescence from each salt sample. Temporal resolution of approximately 200 and 20 ps resulted when the SC operated in the 20 and 2 ns time frames, respectively.

The TPA cross-section was assessed by comparing the fluorescence signal of each salt solution with that of methanol solution of R-6G (the reference) measured under identical experimental conditions and parameters, such as excitation wavelength, pulse duration, bandwidth, average pump power, and fluorescence collection geometry. This use of relative fluorescence relaxes the need for accurate measurement and knowledge of various experimental parameters.

2.4. Toxicity and Cell Imaging. Cell lines and reagents, cell viability measurement (IC-50), cell staining for immunofluorescence imaging, and analysis are described in the Supporting Information.

3. RESULTS AND DISCUSSION

3.1. Synthesis. We synthesized salts **1**−**4** according to Scheme 1 starting from commonly available acetophenones and benzaldehydes. The 1,5-diketones were synthesized from their corresponding acetophenones and benzaldehydes by base-catalyzed aldol condensation reaction followed by the Michael addition reaction on heating in ethanol (EtOH) to reflux. Oxidative cyclization from the respective 1,5-diketones into pyrylium tosylates was achieved on heating at 100 °C with acetic anhydride, *para*-toluenesulfonic acid (TsOH), and triphenylmethanol (Ph_3COH) as the hydride abstractor to facilitate aromatization into the pyrylium tosylates as shown in Scheme 1 (where R and R′ = −H or $-OCH_3$).[21,22]

https://doi.org/10.1021/acs.jpcb.4c03934
J. Phys. Chem. B 2024, 128, 9815−9828

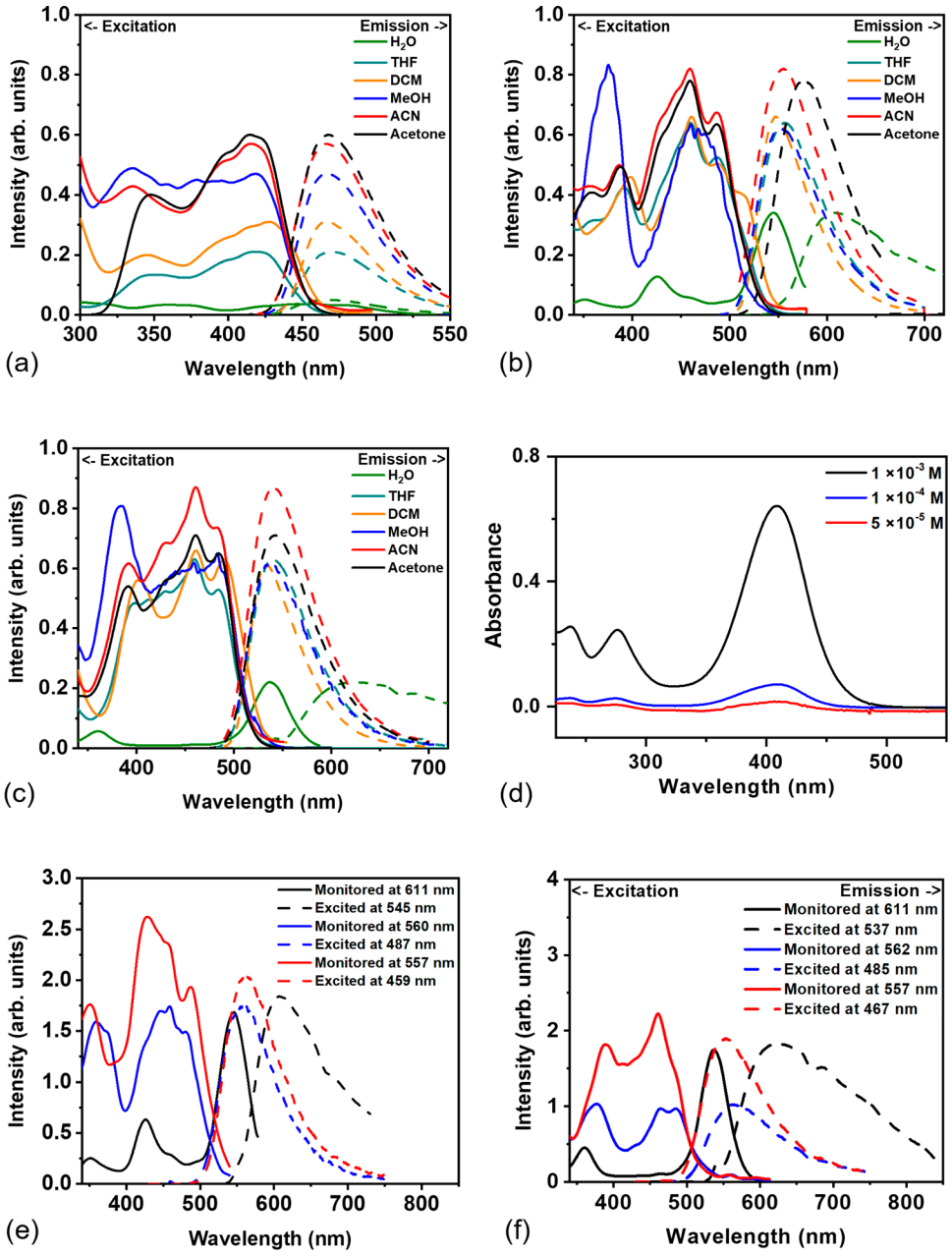

Figure 1. Excitation and emission spectra of salts (a) **1**, (b) **3**, and (c) **4** in different solvents and water; concentration, $C = 1.0 \times 10^{-5}$ M each. Water pH = 1 in (a); and 7 in (b) and (c). (d) Absorption spectra of **2** in water (pH = 7.0); $C = 5.0 \times 10^{-6}$ M (red), 1.0×10^{-4} M (blue), and 1.0×10^{-3} M (black). Excitation and emission spectra of salts (e) **3** and (f) **4** in water (pH = 7.0); $C = 1.0 \times 10^{-5}$ M (red), 1.0×10^{-4} M (blue), and 1.0×10^{-3} M (black).

The 4-(4-methoxyphenyl)-2,6-diphenylpyrylium tosylate was synthesized using a one-pot method by acid-mediated condensation from *para*-methoxybenzaldehyde and acetophenone using TsOH on heating in 1,2-dichloroethane to reflux.[21,22] It is to be noted that its preparation does not require the use of triphenylmethanol. The pseudobases were prepared by ring-opening of the respective pyrylium salts by refluxing in EtOH with sodium acetate trihydrate as the base.[23,35] The chloride salts were prepared by dissolving the respective pseudobases in EtOH with hydrochloric acid to facilitate ring closure.[23,35] Finally, **1**−**4** were synthesized by dissolving the respective chloride salts in acetonitrile (CH_3CN) with ferric chloride ($FeCl_3$) on heating to reflux.[36] In general, perchloric acid and boron trifluoride diethyl etherate are used as common acid catalysts to synthesize pyrylium salts of diverse chemical structures with ClO_4^- or BF_4^- as counterions.[37] However, perchloric acid poses an explosion danger, and boron trifluoride diethyl etherate requires difficult handling, problematic storage, and higher cost. To develop safer, inexpensive, and efficient routes for synthesis of **1**−**4**, we then used tosic acid monohydrate which is a solid, relatively safe to manage, and an inexpensive reagent to synthesize pyrylium tosylate salts. We then successfully converted pyrylium tosylates to pyrylium chlorides using an approach first introduced by Chadwick,[35] and subsequently used by other researchers[38,39] Our modification involving the use of Py-tosylates as starting material instead of Py-perchlorate makes the synthesis safer and easier to manage.

https://doi.org/10.1021/acs.jpcb.4c03934
J. Phys. Chem. B 2024, 128, 9815−9828

Table 1. Optical Spectroscopic Properties of Salts 1, 2, 3, and 4 in Different Solvents (S)[a]

properties	S	salt 1	salt 2	salt 3	salt 4
peak absorption wavelength (nm)	ACN	239, 277, 356, 404	238, 275,415	317, 373, 470	234, 268, 307, 408
$C = 5 \times 10^{-5}$ M	ACT	357, 406	413	374, 417	412
	DCM	242, 282, 370, 417	242, 281, 432	290, 329, 391, 490	239, 276, 314, 426
	THF	363, 410		261, 322, 379, 477	314, 419
	MeOH	277, 358, 406	237, 277,415	320, 377, 474	225, 269, 306, 412
	Water	276, 355, 405	228, 275, 407	275, 317, 372, 469	267, 306, 413
peak emission wavelength (nm)	ACN	466, 467, 470		554, 555, 559	541, 540, 548
$C = 5 \times 10^{-5}$, 1×10^{-4}, and 1×10^{-3} M	ACT	468, 469, 473		557, 555, 561	542, 543, 547
	DCM	466, 468, 484	524, 521, 526	548, 549, 544	533, 537, 545
	THF	471, 472, 474		555, 558, 561	540, 541, 547
	MeOH	467, 466, 480		553, 555, 559	541, 539, 544
	Water	467, 477, 483		557, 560, 611	557, 562, 625
Stokes shift [nm (cm^{-1})]	ACN	62 (3293)		84 (3226)	133 (6026)
$C = 5 \times 10^{-5}$ M	ACT	62 (3263)		140 (6028)	130 (5822)
	DCM	49 (2522)	92 (4064)	58 (2160)	107 (4712)
	THF	61 (3159)		78 (2946)	121 (5348)
	MeOH	61 (3217)		79 (3014)	129 (5788)
	Water	62 (3293)		107 (4269)	97 (3786)
excited state energy [nm (cm^{-1})]	ACN	443 (22,573)		517 (19,342)	506 (19,763)
$C = 5 \times 10^{-5}$ M	ACT	443 (22573)		519 (19,268)	507 (19,724)
	DCM	450 (22,222)	475 (21,053)	525 (19,048)	513 (19,493)
	THF	444 (22,523)		525 (19,048)	508 (19,685)
	MeOH	445 (22,472)		509 (19,646)	505 (19,802)
	Water	441 (22,678)		515 (19,417)	505 (19,802)
FWHM emission bandwidth [nm (cm^{-1})]	ACN	60 (2670)		80 (2519)	75 (2468)
$C = 5 \times 10^{-5}$ M	ACT	65 (2864)		80 (2519)	82 (2686)
	DCM	60 (2670)	120 (4090)	63 (2041)	60 (2026)
	THF	63 (2729)		75 (2339)	70 (1202)
	MeOH	58 (2559)		75 (2381)	77 (2544)
	Water	63 (2799)		95 (2919)	115 (3608)
quantum yield (Φ)[b]	ACN	0.57		0.82	0.87
	ACT	0.60		0.78	0.71
	DCM	0.31	0.16	0.66	0.63
	THF	0.21		0.64	0.63
	MeOH	0.47		0.62	0.64
	Water	0.05		0.34	0.22
fluorescence lifetime (ns)	ACN	2.53 ± 0.02		4.11 ± 0.09	3.59 ± 0.02
$C = 3 \times 10^{-3}$ M	MeOH	1.65 ± 0.01		6.03 ± 0.25	2.79 ± 0.04
	Water			3.81 ± 0.04	
free-running laser operations $C = 3 \times 10^{-3}$ M					
threshold intensity (W/cm^2)	ACN	2.5			0.53
	MeOH	2.13		>5	2
pulse width (ps)	ACN	136 ± 1			128 ± 0.4
	MeOH	118 ± 1			118 ± 1.7
line width (cm^{-1})	ACN	761 ± 5			744 ± 7
	MeOH	446 ± 4			466 ± 5
TP[c] cross-section $\sigma^{(2)}$ (GM)	MeOH	85 ± 16		161 ± 21	401 ± 54
$C = 8 \times 10^{-6}$ M					

[a]Salt solutions in solvents, (S): acetonitrile (ACN), acetone (ACT), dichloromethane (DCM), tetrahydrofuran (THF), methanol (MeOH), and water (pH = 1 for salt **1** and pH = 7 for salts **2**, **3** and **4**). [b]The experimental error in the measured quantum yield values is approximately ±10%. [c]$\sigma^{(2)}$ values for the salts are measured relative to R-6G "standard" of 65 ± 9 GM after ref 46. 1.0 GM = 1.0×10^{-50} cm^4s/photon.

Finally, pyrylium chloride salts were ~~then~~ converted to desired salts **1**−**4** on heating to reflux with $FeCl_3$ in acetonitrile.[36]

Another relatively new method for preparing **1**−**4** starting from the acetophenones and benzaldehydes has been reported[29] and is shown in Scheme S1 for comparison with our method. In this scheme, the 1,5-diketones, prepared also from acetophenones and benzaldehydes, are cyclized in Zn/CH_3COOH under a reductive method to form the corresponding diols followed by dehydration in the presence of hydrochloric acid to afford cyclopentadienes. Subsequently, they are converted to **1**−**4** by a facile C−C bond cleavage of cyclopentadienes with $FeCl_3 \cdot 6H_2O$.[29] Note here that the yields for the last step in the reaction sequences of this method are 42−47%. On the other hand, yields for the last step in our reaction sequences were 66−91%, which were much better than those of the C−C bond cleavage method. Comparing the

https://doi.org/10.1021/acs.jpcb.4c03934
J. Phys. Chem. B 2024, 128, 9815−9828

C−C bond cleavage method for the preparation of **1**−**4**, our Py-Cl method is more general and robust for the preparation of Py-salts that have been developed for more than a century. Furthermore, our method is also suitable for the synthesis of other anionic chloro complexes of Zn (II), Sn (II), Pb (II), Cd (II), Au (III), and Pt (IV),[35] which the C−C bond cleavage method may not be suited for.[29]

3.2. Solubility. *3.2.1. Solubility in Common Organic Solvents.* Pyrylium salts of diverse chemical structures are generally prepared with counterions ClO_4^-, BF_4^-, PF_6^-, and TsO^-. They contain hydrophobic, bulky counterions that generally have limited solubility in organic solvents such as ACN and DCM.[40] However, salts **1**−**4** were highly soluble (concentration ~10^{-3} M) in acetone, ACN, methanol, DCM, and tetrahydrofuran (THF) with the exception of **2** which was insoluble in THF. Their high solubility in organic solvents is related to the $FeCl_4^-$ for **1**; and to the combination $FeCl_4^-$ and methoxy group(s) for **2**−**4**. We conclude that the substituent methoxy group in the para-position of the 2-, 4-, and 6-phenyl rings of these salts in combination with $FeCl_4^-$ significantly increased the solubility of these salts.

3.2.2. Solubility in Water. As discussed in the Introduction, Py-salts are inherently unstable in water and tend to become stable only in acidic water (pH < 3). Salt **1** was found to be highly soluble (concentration ~10^{-3} M) in acidic water (pH = 1). In contrast, salt **2** was highly soluble (~10^{-3} M) in water (pH = 7) as shown in Figure 1d. Interestingly, the introduction of a single methoxy group in the para-position of the 4-phenyl ring made this Py-salt stable in water solution. As we introduced two methoxy groups in the para-positions of 2- and 6- phenyl rings of salt **3**; and three methoxy groups in the para-positions of 2-, 4-, and 6-phenyl rings of salt **4**, both the salts became highly soluble (concentration ~10^{-3} M) and stable in water (pH = 7) as shown in Figure 1e,f, respectively. Solubility and stability of the salts in water have useful implications in biomedical imaging and photodynamic therapy applications. To our knowledge, salts **2**, **3**, and **4** have the highest solubility in water among the Py-salts and do not suffer from the inherent instability (ring opening) of other Py-salts.[41,42] Resta et al.[41] demonstrated that the methoxy groups in the para-positions of 2- and 6-phenyl rings cause the stability of styrylpyrylium salts with BF_4^- counterion in water. Wen et al.[42] showed that when amino groups are introduced in the para-positions of 2- and 6-phenyl rings in the rigidified Py-salts with ClO_4^- counterion, the salts become stable in water. These experimental results are also in excellent agreement with theoretical studies using density functional theory calculations.[41] These studies suggested that C-2 and C-6 of the pyrylium moiety (where two phenyl rings are attached) are the most electron-deficient positions, implying that nucleophilic attack by water at these sites is responsible for the instability of Py-salts in water solution. Thus, by the introduction of electron-donating groups such as methoxy and amino groups at the 2- and/or 6-positions of Py-salts, their chemical stability in water may be improved significantly.

3.3. Optical Spectroscopic Properties. The fluorescence spectra (right) and excitation spectra (left) of salts **1**, **3**, and **4** dissolved in different organic solvents—acetone, acetonitrile (ACN), methanol (MeOH), tetrahydrofuran (THF), dichloromethane (DCM), and water (pH = 1.0, and pH = 7.0) at room temperature are displayed in Figure 1. Table 1 summarizes the key spectroscopic characteristics that include absorption peak positions, fluorescence peak position, Stokes shifts in various solvents, quantum yield, and fluorescence lifetime. Table S1 provides the molar extinction coefficients of the salts in different solvents.

The salt solutions absorb light strongly in the 300−500 nm wavelength range and fluoresce with high quantum efficiency between 500−700 nm. The absorption (excitation) spectra are structured with multiple absorption peaks. The lowest-energy (longest wavelengths) absorption band in each salt is attributed to the $S_0 \rightarrow S_1$ transition, while the higher-energy absorption bands belong to transitions from S_0 to other higher-lying states.

The fluorescence spectra of every salt solution in different solvents consist of a single, broad Stokes-shifted band, which is attributed to $S_1 \rightarrow S_0$ vibronic transitions. As listed in Table 1, the solutions of salts **1**, **3**, and **4** exhibit Stokes shifts of approximately 49 nm (2522 cm^{-1}) to 133 nm (6026 cm^{-1}) and emission bandwidths of 58 nm (2559 cm^{-1}) to 115 nm (3608 cm^{-1}). Each of these two parameters shows significant solvent-dependent variations for salt **3** and salt **4**, but only minor variations for salt **1**.

Salt **2** is highly soluble in water and other organic solvents, except THF. However, it does not fluoresce appreciably in any of these solvents other than in DCM with a modest quantum yield of 0.16. Quantum yields of salt **3** and salt **4** are substantially higher in most of the solvents listed in Table 1, and reach values as high as 0.82 and 0.87, respectively in acetonitrile solutions. As a comparison we note that two of the styrylpyrylium salts with BF_4^- show higher quantum yields in DCM (0.59 and 0.54) than in acetonitrile (0.38 and 0.28) and the lowest quantum yields (0.03 and 0.01) in phosphate-buffered solutions (PBS) pH = 7.4.[41] In contrast, our salts **1**, **3**, and **4** showed the highest quantum yields in acetonitrile than in DCM as presented in Table 1. The lowest quantum yields were 0.05 for **1** in acidic water (pH = 1); and 0.34 and 0.22 for **3** and **4**, respectively, in water (pH = 7). Interestingly, **3** and **4** showed appreciably much higher quantum yields in water when compared with other water-soluble red-fluorescent dyes for two-photon deep-tissue imaging, such as 2,5-dimethoxy-1,4-bis{2-[1-[2-[2-(2-hydroxyethoxy)ethoxy]-ethyl]-pyridin-1-iumyl]ethenyl}benzene chloride and 2,5-dimethoxy-1,4-bis{1-[2-[2-(2-hydroxyethoxy)ethoxy]ethyl]-4-(1,3-butadien-1-yl)-pyrinium}benzene iodide.[43] Generally, most of the dyes show much higher quantum yields in organic solvents than in water.[43] Two of the rigidified Py-salts ClO_4^- show high quantum yields 0.33 and 0.51 in ethanol and 0.16 and 0.21 in PBS (pH = 7.4) solutions.[42] The measured high quantum yields of **3** and **4** in organic solvents as well as in water suggest that Py-salts with $FeCl_4^-$ counterions and having electron-donating groups without a rigidification protocol can be a useful design strategy for the synthesis of the salts with high quantum yields. These results have implications for their fluorescence and nonlinear optical properties as discussed in the subsequent section.

The fluorescence properties of Py-salts generally depend on the nature of substituents in the 2-, 4-, and 6-phenyl groups of the salts and the influence of the solvents. In this regard, many Py-salts are considered as bichromophoric fluorescent molecules with a distinct *x*-axis passing through the 2- and 6- positions of the phenyl groups, and a *y*-axis that passes through the 4-position of the phenyl group.[40] Depending on the structure of the salt, transitions involving the chromophores along the *x*-axis (or, *y*-axis) may dominate the fluorescence. With this picture in mind the differences between

https://doi.org/10.1021/acs.jpcb.4c03934
J. Phys. Chem. B 2024, 128, 9815−9828

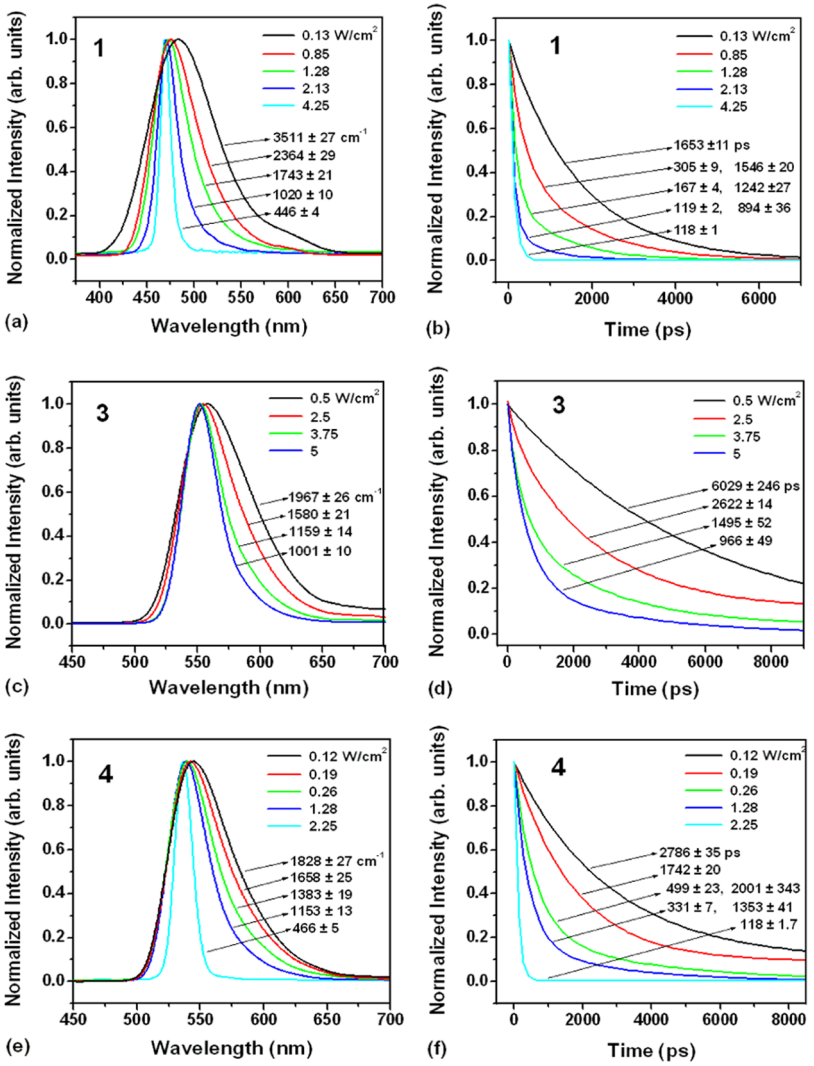

Figure 2. Pump intensity-dependent fluorescence spectra and fluorescence decay time: (a, b) of salt **1**; (c, d) of salt **3**; and (e, f) for salt **4** in methanol (concentration ~3.0×10^{-3} M) for pulsed excitation using light of wavelength 400 nm.

the fluorescence properties of the salts, in particular, the lower fluorescence quantum yield of salt **2** compared to those of **1**, **3**, and **4** may be explained. Salt **2** with a methoxy group attached to the 4-phenyl group is a strong acceptor (*y*-chromophore) that allows for the formation of nonradiative twisted intramolecular charge transfer (TICT) states more favorably than the structures of Salt **3** with methoxy groups attached to the 2-, 6-phenyl groups, and Salt **4** with methoxy groups attached to the 2-, 4- and 6-phenyl groups. Salt **4** is thus highly symmetric and so is Salt **1** with no methoxy groups attached.

From measurements of quantum yields of different Py-salts with various substituents at different positions, it is well established that Py-salts having substituents attached to the 2- and 6-phenyl groups (*x*-chromophore) have much higher quantum yields as the fluorescence transition occurs from the equilibrated S_1 state to the Franck–Condon S_0 state.[40] For example, 4-(4-methoxyphenyl)-2,6-diphenylpyrylium salt with a ClO_4^- counterion has a fluorescence quantum yield of 0.28 in DCM, but it does not fluoresce at all in acetonitrile. The absence of fluorescence in acetonitrile suggests that the high polarity of this solvent strongly favors the formation of nonradiative TICT, *i.e.*, quenching occurs when compared with a nonpolar solvent such as DCM. In contrast, 2,6-bis(4-methoxyphenyl)-4-phenylpyrylium salt (*x*-chromophore) with ClO_4^- has high quantum yields of 0.95 and 0.82 in DCM and acetonitrile, respectively. Additionally, 2,4,6-tris(4-methoxyphenyl)pyrylium salt with ClO_4^- (highly symmetric as salt **4**) also has high quantum yields of 0.95 and 0.97 in DCM and acetonitrile, respectively.[40] The situation in the above examples is strikingly similar to our salts **2**, **3**, and **4**. The formation of nonradiative TICT states in salt **2** helps explain its significant difference in fluorescence properties with the other three salts.

3.4. Fluorescence Dynamics and Lasing Potential. The time-resolved and excitation intensity-dependent measurements of the fluorescence dynamics and spectra of the solutions of salts **1**, **3**, and **4** in acetonitrile and methanol at room temperature for pulsed excitation using light of wavelength 400 nm was conducted to extract fluorescence lifetime and assess their potential as active materials for dye lasers.[20−23] These two solvents were chosen as they are safer, provide high fluorescence quantum yields for the salts, and are commonly used for dye laser applications. Figure 2b,d,f presents the time-resolved fluorescence decay dynamics as a function of the average excitation intensity of the methanol solution of salts **1**, **3**, and **4**, respectively. Corresponding

https://doi.org/10.1021/acs.jpcb.4c03934
J. Phys. Chem. B 2024, 128, 9815−9828

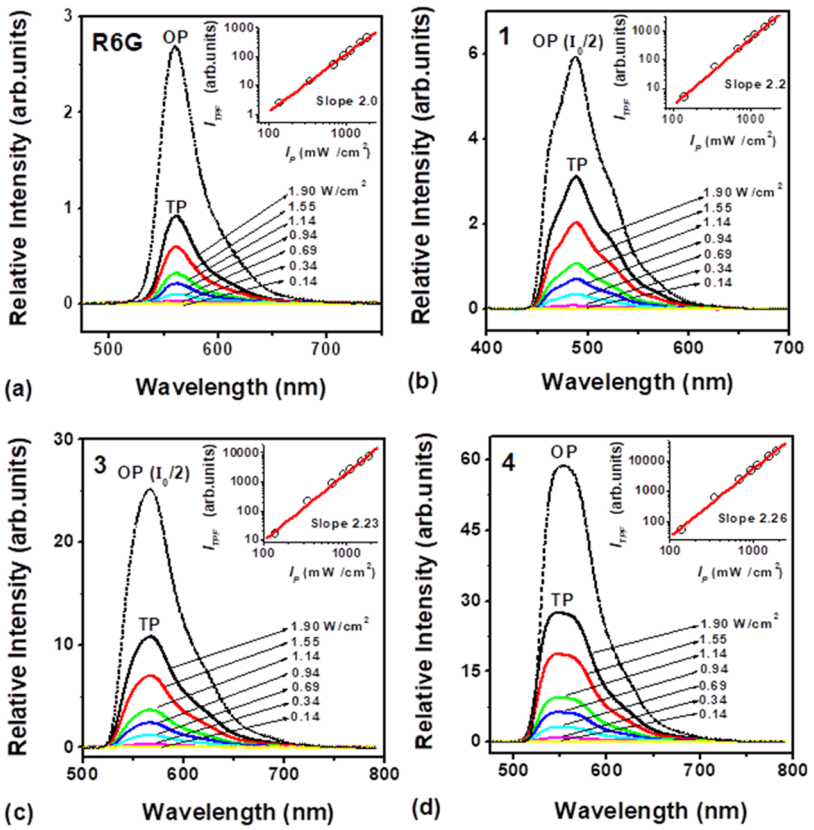

Figure 3. Two-photon absorption-induced fluorescence (TPAIF) spectra of (a) R-6G (~1×10^{-4} M solution) as a reference, (b) salt **1**, (c) salt **3**, and (d) salt **4** in methanol (~3×10^{-3} M solutions for salt **1**, **3**, and **4**). One-photon (OP) fluorescence spectra at 400 nm excitation are superimposed for comparison of TP and OP fluorescence spectral shapes.

average excitation intensity-dependent fluorescence spectra are displayed in Figure 2a,c,e, respectively.

The salient features of the fluorescence decay curves and the corresponding spectra are as follows. For low average pump intensity (~0.13 W/cm^2) salt **1** fluorescence [black curve, Figure 2b] decayed as a single exponential with a decay time of 1.65 ± 0.01 ns. The corresponding emission spectrum (black curve, Figure 2a) has a fwhm line width of 3511 ± 27 cm^{-1} (81.6 ± 1.2 nm). As the average excitation intensity was increased, a faster component of emission was observed in addition to the longer component and the decay curve was no longer a single exponential. A corresponding shortening of the emission line width was observed.

As a typical example, for the average excitation intensity of 0.85 W/cm^2, [red curve in Figure 2b] a double exponential fit of the form, $I(t) = I_L \exp(-t/\tau_L) + I_S \exp(-t/\tau_S)$, to the data provided a shorter decay time of τ_S = 305 ± 9 ps and a longer-decay time of 1546 ± 20 ps, where I, I_L and I_S are the normalized values of the total intensity, intensity of the longer-decay component and intensity of the shorter-decay component, respectively. The corresponding spectrum [red curve in Figure 2a] has an fwhm line width of 2364 ± 29 cm^{-1}.

The longer fluorescence lifetime and wider bandwidth at low pump intensity are indicative of spontaneous emission, while a shorter lifetime and narrower bandwidth at higher excitation intensities are consistent with amplified spontaneous emission (ASE) and stimulated emission. Another consequence of increasing pump intensity is the enhancement of I_S and detraction of I_L. At the average pump intensity of ~2.13 W/cm^2 the shorter decay time reduced to 119 ± 12 ps and the bandwidth narrowed to 1020 ± 10 cm^{-1} (24.0 ± 0.3 nm). Stimulated emission is the dominant decay mechanism at this excitation intensity, and spontaneous emission appears as a weak long tail in the decay profile. At this point when the orientation of the cuvette was slightly adjusted to feedback, a fraction of the emission reflected by the cuvette sidewalls through the pumped volume and pump intensity was increased to 4.25 W/cm^2 free-running laser action was observed. The spot size of the emission tightened and became intense and significantly directional with a concomitant shorter pulse width of 118 ± 11 ps (Figure 2b, neon color curve) and line width of 446 ± 4 cm^{-1} (11.3 ± 0.1 nm) [Figure 2a, neon curve].

Similar pump intensity-dependent bandwidth narrowing (from 1828 ± 27 to 466 ± 5 cm^{-1}) and lifetime shortening (from 2.8 ns to 118 ps) and free-running laser action were also observed in a methanol solution of salt **4**, as displayed in Figure 2e,f, respectively. While the line widths of 446 cm^{-1} (or, 466 cm^{-1}) are much shorter than the corresponding fluorescence line widths, those are rather broad for a laser line. These broader line widths are expected since no wavelength selection element was used in the cavity, salt concentration was high, and the optical gain of the salt solution, like organic dyes, was high enough to support broadband lasing. The methanol solution of salt **3** also exhibited some line width narrowing and decay-time shortening, as shown in Figure 2c,d, respectively but free-running laser action was not observed. We attribute this behavior to the fact that the pump wavelength of 400 nm used in this experiment is not well suited for exciting this salt solution. Pumping at a more optimal wavelength that can excite at or

https://doi.org/10.1021/acs.jpcb.4c03934
J. Phys. Chem. B 2024, 128, 9815−9828

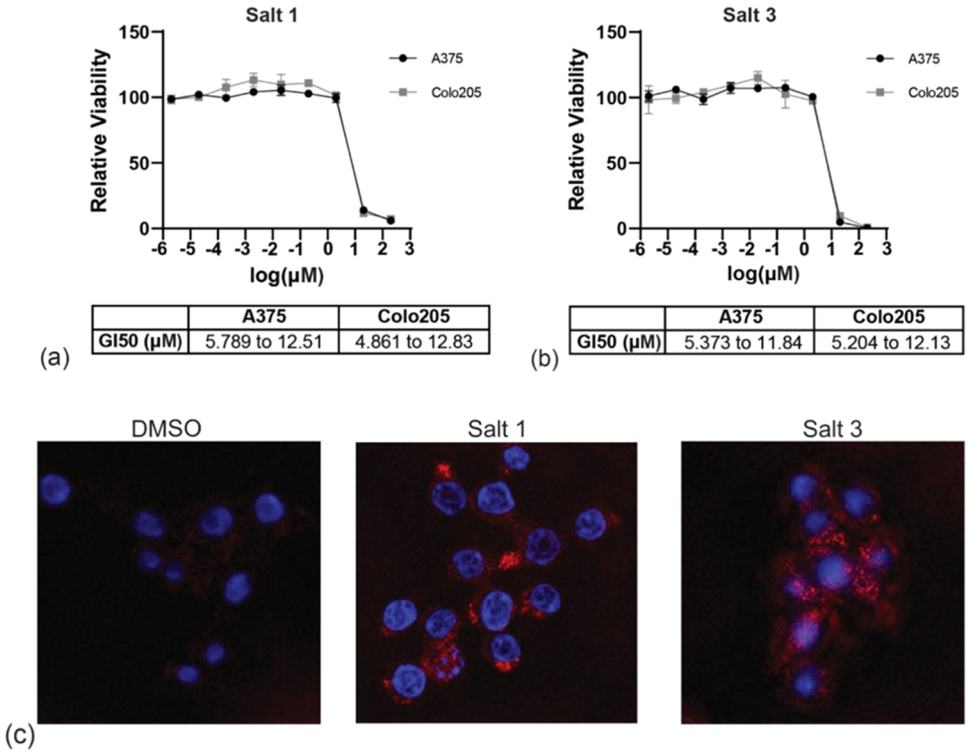

	A375	Colo205
GI50 (μM)	5.789 to 12.51	4.861 to 12.83

	A375	Colo205
GI50 (μM)	5.373 to 11.84	5.204 to 12.13

Figure 4. Toxicity and imaging of pyrylium tetrachloroferrates in human cells. Cell viability measurements in A375 and Colo205 cells following treatment with increasing doses of (a) salt **1** and (b) salt **3** for 72 h. GI50 values are reported as 95% confidence intervals. (c) Representative immunofluorescent images of RKO cells intracellularly stained with 1 μM salt **1** or salt **3** for 1 h (red). Hoechst dye (blue) was used to stain the nucleus. DMSO-treated RKO cells were used as a negative control.

near the peak of the lowest absorption band of the salt solution may lead to laser action in it as well and is planned to be pursued.

Similar excitation intensity-dependent fluorescence decay-time shortening, bandwidth narrowing, and free-running laser action are observed using acetonitrile solutions of salt **1** and salt **4** and are displayed in Figure S16. The key results from these measurements, such as fluorescence lifetime, pulse width, bandwidth, and threshold for laser operation, are listed in Table 1. It should be noted that the lowest pulse width, bandwidth, and free-running laser action are attained at significantly lower average pump intensities for the acetonitrile solution of salts **1** and **4** than those for the corresponding methanol solutions. The fractional values of the long decay component (I_L) and short decay component (I_S) as a function of average pump intensity for salts **1**, **3**, and **4** in methanol are presented in Table S2.

The room temperature fluorescence spectrum of a DCM solution of salt **2** (concentration 0.1 mM) spanned from 450–750 nm with a peak at 547 nm (Figure S17a), and the fluorescence lifetime was measured as 4.32 ± 0.18 ns (Figure S17b). It is to be noted that the salt fluoresced only in DCM and in no other solvents.

3.5. Two-Photon Absorption-Induced Fluorescence. We investigated the two-photon absorption-induced fluorescence (TPAIF) from the solutions of Py-tetrachloroferrate salts **1**, **3**, and **4** in methanol and acetonitrile to explore the feasibility of their application as contrast agents for two-photon imaging and microscopy and other applications. Figure 3b–d displays the TPAIF spectra of the methanol solutions of the salts **1**, **3**, and **4**, respectively, at several excitation intensities. Figure 3a presents the TPAIF spectra of a methanol solution of R-6G, which is used as a reference to estimate the TPA cross-section. Other than the increase in the signal amplitude with increasing average intensity of the 800 nm pump beam, the TP fluorescence spectra had similar shape and spectral range. The TP fluorescence spectra have similar features and structures as the one-photon fluorescence spectra excited by 400 nm frequency-doubled output of the 800 nm beam indicating that the fluorescence transitions originate from the same excited state in both cases. The logarithmic plots of the fluorescence intensity vs average pump intensity, shown in the insets of Figure 3, are linear with a slope of approximately 2.0, as expected for the quadratic dependence of fluorescence intensity on pump power in a two-photon excitation process. The TP fluorescence spectra of the acetonitrile solutions of the salts are presented in Figure S18. It is interesting to note that the salt **3** solution in water (pH = 7) showed significant TPAIF (Figure S19), which is very encouraging for its application as a contrast agent in two-photon microscopy and two-photon fluorescence imaging of biomedical specimens. Toxicity and cell imaging studies (section 3.6 below) also indicate its viability for biological and medical applications.

The TPA cross-sections of the salt solutions in methanol were estimated in reference to that of Rhodamine 590 and R-6G solution in methanol with known TPA cross-section following a well-established relative measurement procedure that avoids complications associated with absolute measurement of fluorescence.[32,44−46] These complications include rather precise knowledge of pulse width, bandwidth, temporal coherence, and profile of the pump beam.[32,43] The results, presented in Table 1, indicate that the TPA cross sections of salt **1** (85 ± 16 GM) salt **3** (161 ± 21 GM), and salt **4** (401 ± 54 GM) are substantially larger than 65 ± 9 GM for R-6G.[46]

https://doi.org/10.1021/acs.jpcb.4c03934
J. Phys. Chem. B 2024, 128, 9815−9828

The TPA cross sections of Salts **3** and **4** are higher than that of Salt **1** by a factor of 2 and 5, respectively. We tentatively ascribe this variation to the structural differences between the salts described earlier, which lead to differences in their vibronic energy level structures. The vibronic couplings are also influenced by the solvent. TPA transition rate depends on all intermediate states, so the cross sections depend significantly on the vibronic energy level structure. It should be noted that such variations in different related dyes are common. For example, the TPA cross sections of R-6G, Rhodamine-B, Rhodamine-101 vary approximately within a factor of 4−11 depending on the solvent.[45]

3.6. Toxicity and Cell Imaging. We sought to explore the potential biological and biomedical imaging applications of salts **1**, **3**, and **4**. First, we assessed the toxicity profile of the compounds in human cancer cell lines. A375 melanoma and Colo205 colorectal carcinoma cells were treated with salts **1** and **3** for 3 days before cellular viability was measured (Figure 4a,b). Both tested salts demonstrated 50% growth inhibition concentration (GI50) in the range 5−12 μM (Figure 4a,b).

Based on recent findings of organic salts showing fluoresecence activity in cellular models,[47,48] we wanted to explore if our pyrylium tetrachloroferrate salts would function as cellular fluorophores. RKO colorectal carcinoma cells were intracellularly stained with salt **1** or salt **3** before being subjected to immunofluorescence imaging. After excitation with a 633 nm laser beam, both salts **1** and **3** showed increased intracellular fluorescence intensity when compared to our DMSO-treated controls (Figure 4c). With similar protocols, we tried to use salt **4** and it did not produce satisfactory results (data not shown), which suggests it may be intracellularly less stable compared to salts **1** and **3**. Taken together, salts **1** and **3** function as cellular fluorophores *in vitro* and have no adverse effects on the cellular viability in nanomolar ranges.

The applications of these new cellular fluorophores (Salts **1** and **3**) deserve further elaboration. Each fluorophore available on the market has limitations regarding what it binds and in what wavelengths it is active in. These limitations become the most apparent when staining cells with multiple fluorophores during flow cytometry and immunofluorescence imaging, as overlap in cellular binding locations or wavelength activity prevents accurate interpretation of the signal. Therefore, there is a need to discover new cellular fluorophores with wide-ranging fluorescence activity that bind to unique cellular substrates. Based on the above data, Salts **1** and **3** would be compatible with blue or green cellular fluorophores to achieve high-resolution multiplex cellular imaging, which is relevant for many molecular biology applications.

High TPA cross-section and strong TPA-induced fluorescence also make Salts **1** and **3** suitable as contrast agents for two-photon imaging and two-photon microscopy of biological tissues.[44,49] Biological tissues scatter light strongly, and native tissue fluorophores absorb light in the 400−500 nm and near-ultraviolet wavelengths. So, one-photon absorption-based imaging and microscopy of thick tissues is limited by low penetration depth, strong background from tissue fluorescence, and low resolution. Two-photon excitation of contrast agents (such as Salts **1** and **3**) requires simultaneous absorption of two near-infrared (NIR) photons commonly in the 750−1050 nm range. Light in this wavelength range is not absorbed by native tissue fluorophores and is scattered to a lesser degree than the visible light by biological tissues, allowing deeper penetration. Since TPA depends quadratically on the excitation beam intensity and requires the use of a focused beam of NIR light, the fluorescence signal arises predominantly from the focal volume, resulting in high spatial resolution and optical sectioning effect.

4. CONCLUSIONS

Four pyrylium salts with $FeCl_4^-$ counterions have been synthesized for light emitting, biomedical imaging, and nonlinear optical (NLO) applications. The salts are stable and dissolve at high concentrations in common organic solvents and water. Water stability of these Py-salts is attributed to the presence of $FeCl_4^-$ as the counterion in all four salts, and in addition the attachment of the methoxy group(s) to the phenyl group(s) in salts **2**, **3**, and **4**. Solutions of the salts in common organic solvents absorb light strongly in the blue-green and near-ultraviolet spectral ranges and fluoresce with high quantum efficiency in the green-red spectral region. Under intense short-pulsed laser excitation solutions of two of these salts (**1** and **4**) in methanol and acetonitrile exhibit stimulated emission and free-running laser action. Three of the salts (**1**, **3**, and **4**) have significantly high two-photon absorption cross-section. Toxicity and cell imaging studies suggest that two of the salts (**1** and **3**) have no harmful effects on cellular viability and may be used as contrast agents for biomedical imaging. So, those would be compatible with blue or green cellular fluorophores to achieve high-resolution multiplex cellular imaging, which is relevant for many molecular biology applications. Combined with strong two-photon fluorescence, these cell imaging results further promise high-resolution NLO deep-tissue imaging using these salts as contrast agents. Finally, the synthesized pyrylium salts with $FeCl_4^-$ counterions provide promising opportunities for diverse applications, including light emission, biomedical imaging, and nonlinear optics. Their stability, solubility in both organic solvents and water, and recently reported piezochromic properties,[50] combined with their high quantum efficiency fluorescence and significant two-photon absorption cross-section, make them valuable candidates for advancing both fundamental research and practical applications in organic−inorganic hybrid materials.[51−53]

■ ASSOCIATED CONTENT

Supporting Information

The Supporting Information is available free of charge at https://pubs.acs.org/doi/10.1021/acs.jpcb.4c03934.

Detailed synthesis and characterization of precursors to **1**−**4**; ^{1}H and ^{13}C NMR spectra of precursors; FTIR and Raman spectra of **1**−**4**; molar absorptivity of **1**−**4** in Table S1; pump intensity-dependent fluorescence spectra and decay curves of **1** and **4** in acetonitrile; fractional values of the long decay component (I_L) and short decay component (I_S) as a function of average pump intensity for salts **1**, **3**, and **4** in Table S2; absorption and fluorescence spectra of **2** in DCM and its fluorescence decay curve; TPAIF spectra of **1**, **3**, and **4** in acetonitrile; TPAIF spectra of **3** in water; cell viability measurement; and cell staining for immunofluorescence imaging and analysis. (PDF)

https://doi.org/10.1021/acs.jpcb.4c03934
J. Phys. Chem. B 2024, 128, 9815−9828

AUTHOR INFORMATION

Corresponding Author

Pradip K. Bhowmik − *Department of Chemistry and Biochemistry, University of Nevada Las Vegas, Las Vegas, Nevada 89154, United States;* orcid.org/0000-0002-7737-9317; Email: pradip.bhowmik@unlv.edu

Authors

David King − *Department of Chemistry and Biochemistry, University of Nevada Las Vegas, Las Vegas, Nevada 89154, United States*

Si L. Chen − *Department of Chemistry and Biochemistry, University of Nevada Las Vegas, Las Vegas, Nevada 89154, United States*

Ronald Carlo G. Principe − *Department of Chemistry and Biochemistry, University of Nevada Las Vegas, Las Vegas, Nevada 89154, United States*

Haesook Han − *Department of Chemistry and Biochemistry, University of Nevada Las Vegas, Las Vegas, Nevada 89154, United States*

Egor Evlyukhin − *Department of Physics and Astronomy, University of Nevada Las Vegas, Las Vegas, Nevada 89154, United States*

Petrika Cifligu − *Department of Physics and Astronomy, University of Nevada Las Vegas, Las Vegas, Nevada 89154, United States*

Ahamed Jubair − *Department of Physics, Center for Discovery and Innovation, The City College of New York, New York, New York 10031, United States; Physics Program, The Graduate Center, City University of New York (CUNY), New York, New York 10016, United States*

Vladimir Kartazaev − *Department of Physics, Center for Discovery and Innovation, The City College of New York, New York, New York 10031, United States*

Swapan K. Gayen − *Department of Physics, Center for Discovery and Innovation, The City College of New York, New York, New York 10031, United States; Physics Program, The Graduate Center, City University of New York (CUNY), New York, New York 10016, United States*

Shane T. Killarney − *Department of Pharmacology and Cancer Biology, Duke University, Durham, North Carolina 27705, United States*

Julia D. Caci − *Department of Pharmacology and Cancer Biology, Duke University, Durham, North Carolina 27705, United States*

Kris C. Wood − *Department of Pharmacology and Cancer Biology, Duke University, Durham, North Carolina 27705, United States*

Complete contact information is available at: https://pubs.acs.org/10.1021/acs.jpcb.4c03934

Notes

The authors declare no competing financial interest.

ACKNOWLEDGMENTS

P.K.B. and E.E. sincerely acknowledge the financial support of an industrial-sponsored project supported by Koshee Company, Las Vegas, USA. P.K.B. sincerely acknowledges the Knowledge Fund that is administered by the Nevada Governor's Office of Economic Development (GOED) and the University of Nevada Las Vegas (UNLV). H.H. sincerely acknowledges the Faculty Opportunity Award (FOA) that is administered by the Office of Sponsored Programs (OSP) at UNLV. E.E. and P.C. sincerely acknowledge support from the US Department of Energy, the Basic Energy Sciences (BES) program under Award Number DE-SC0023248. A portion of this work was performed at GeoSoilEnviroCARS (The University of Chicago, Sector 13), Advanced Photon Source, Argonne National Laboratory. GeoSoilEnviroCARS is supported by the National Science Foundation − Earth Sciences via SEES: Synchrotron Earth and Environmental Science (EAR − 2223273). This research used resources from the Advanced Photon Source, a US Department of Energy (DOE) Office of Science User Facility operated for the DOE Office of Science by Argonne National Laboratory under Contract No. DE-AC02-06CH11357. The use of the GSECARS Raman Lab System was supported by the NSF MRI Proposal (EAR-1531583). The work at the City College of New York (A.J., V.K., and S.K.G.) is supported in part by NSF Grant No. HRD-2112550 (Phase II CREST IDEALS).

REFERENCES

(1) Trudel, S. Oranic electronic. *Phys. Today* **2023**, *76* (12), 24−30.

(2) McCulloch, I.; Chabinyc, M.; Brabec, C.; Nielsen, C. B.; Watkins, S. E. Sustainability considerations for organic electronic products. *Nat. Mater.* **2023**, *22*, 1304−1310.

(3) Li, Y.; Wang, H.; Li, X. Over one century after discovery: pyrylium salt chemistry emerging as a powerful approach for the construction of complex macrocycles and metallosupramolecules. *Chem. Sci.* **2020**, *11*, 12249−12268.

(4) Sideri, I. K.; Voutyritsa, E.; Kokotos, C. G. Photoorganocatalysis, small organic molecules and light in the service of organic synthesis: the awakening of a sleeping giant. *Org. Biomol. Chem.* **2018**, *16*, 4596−4614.

(5) Miranda, M. A.; Garcia, H. 2,4,6-Triphenylpyrylium tetrafluoroborate as an electron-transfer photosensitizer. *Chem. Rev.* **1994**, *94*, 1063−1089.

(6) Hola, E.; Ortyl, J. Pyrylium salt as a visible-light-induced photoredox catalyst for polymer and organic synthesis − perspectives on catalyst design and performance. *Eur. Polym. J.* **2021**, *150*, 110365.

(7) Ogawa, K. A.; Goetz, A. E.; Boydston, A. J. Metal-free ring-opening metathesis polymerization. *J. Am. Chem. Soc.* **2015**, *137*, 1400−1403.

(8) Rao, B. A.; Lee, J.-Y.; Son, Y.-A. Synthesis of a novel pyrylium salt with chemoselectivity to a cyanide anion. *Supramol. Chem.* **2015**, *27*, 191−200.

(9) Beltrán, A.; Burguete, M. I.; Abánades, D. R.; Pérez-Sala, D.; Luis, S. V.; Galindo, F. Turn-on fluorescent probes for nitric oxide sensing based on the ortho-hydroxyamino structure showing no interference with dehydroascorbic acid. *Chem. Commun.* **2014**, *50*, 3579−3581.

(10) Wetzl, B. K.; Yarmoluk, S. M.; Craig, D. B.; Welfbeis, O. S. Chameleon labels for staining and quantifying protein. *Angew. Chem., Int. Ed.* **2004**, *43*, 5400−5402.

(11) Terkia-Derdra, N.; Andreu, R.; Sallé, M.; Levillain, E.; Orduna, J.; Garín, J.; Ortí, E.; Viruela, R.; Pou-AméRigo, R.; Sahraoui, B.; Gorgues, A.; Favard, J.-F.; Riou, A. π Conjugation across the tetrathiafulvalene core: Synthesis of extended tetrathiafulvalene derivatives and theoretical analysis of their unusual electrochemical properties. *Chem. − Eur. J.* **2000**, *6*, 1199−1213.

(12) Mysliwiec, J.; Snitch, L.; Bartkiewicz, S.; Mankiewicz, A.; Essaidi, Z.; Kajzar, F.; Sahraoui, B. Amplified spontaneous emission in the spiropyran-biopolymer based system. *Appl. Phys. Lett.* **2009**, *94*, No. 241106, DOI: 10.1063/1.3155203.

(13) Zongo, S.; Kerasidou, A. P.; Sone, B. T.; Diallo, A.; Mthunzi, P.; Iliopoulos, K.; Nkosi, M.; Maaza, M.; Sahraoui, B. Nonlinear optical properties of poly(methyl methacrylate) thin films doped with Bixa Orellana dye. *Appl. Surf. Sci.* **2015**, *340*, 72−77.

(14) Gu, C.; Zhang, H.; You, P.; Zhang, Q.; Luo, G.; Shen, Q.; Wang, Z.; Hu, J. Giant and multistage nonlinear optical response in porphyrin-based surface-supported metal−organic framework nanofilms. *Nano Lett.* **2019**, *19*, 9095−9101.
(15) Zawadzka, A.; Waszkowska, K.; Karakas, A.; Płóciennik, P.; Korcala, A.; Wisniewski, K.; Karakaya, M.; Sahraoui, B. Diagnostic and control of linear and nonlinear optical effects in selected self-assembled metallophthalocyanine chlorides nanostructures. *Dyes Pigm.* **2018**, *157*, 151−162.
(16) Waszkowska, K.; Cheret, Y.; Guichaoua, D.; Travers, T.; El-Ghayoury, A.; Gindre, D.; Göring, P.; Lelonek, M.; Andrushchak, A.; Goncharova, I.; Sahraoui, B. Enhanced nonlinearities in hybrid structure based on nanoporous membrane and a metallohelicate with promising application in nanophotonics and NLO. *Opt. Lett.* **2023**, *48*, 2897−2900.
(17) Schäfer, F.; Schmidt, W.; Marth, K. New dye lasers covering the visible spectrum. *Phys. Lett. A* **1967**, *24*, 280−281.
(18) Tripathi, S.; Wintgens, V.; Valat, P.; Toscano, V.; Kossanyi, J.; Bos, F. Laser effect of a series of variously substituted pyrylium and thiopyrylium salts. *J. Lumin.* **1987**, *37*, 149−157.
(19) Kotowski, T.; Skubiszak, W.; Soroka, J. A.; Soroka, K. B.; Stacewicz, T. Pyrylium and thiopyrylium high efficiency dyes. *J. Lumin.* **1991**, *50*, 39−45.
(20) Fakis, M.; Polyzos, J.; Tsigaridas, G.; Parthenios, J.; Fragos, A.; Giannetas, V.; Persephonis, P.; Mikroyannidis, J. Novel class of pyrylium dyes with high efficiency in lasing and two-photon absorption fluorescence. *Chem. Phys. Lett.* **2000**, *323*, 111−116.
(21) Koh, J. J.; Lee, C. I.; Ciulei, M. A.; Han, H.; Bhowmik, P. K.; Kartazaev, V.; Gayen, S. K. Synthesis, optical spectroscopy, and laser potential of pyrylium tosylates. *J. Mol. Struct.* **2018**, *1171*, 458−465.
(22) Bhowmik, P. K.; Lee, C. I.; Koh, J. J.; Han, H.; Jubair, A.; Kartazaev, V.; Gayen, S. K. Synthesis, optical, and thermal properties of 2,4,6-tris(4-substituted phenyl)pyrylium tosylates and triflimides. *J. Mol. Struct.* **2020**, *1202*, No. 127325.
(23) Bhowmik, P. K.; Principe, R. C. G.; Chen, S. L.; King, D.; Han, H.; A Jubair, A.; V Kartazaev, V.; Gayen, S. K. Synthesis, optical spectroscopy, and laser potential of 2,4,6-triphenylpyrylium chloride. *Chem. Phys. Lett.* **2022**, *805*, No. 139927.
(24) Dinculescu, A.; Balaban, T. S.; Popescu, C.; Toader, D.; Balaban, A. T. Synthesis of pyrylium salts with various anions. *Bull. Soc. Chim. Belg.* **1991**, *100*, 665−672.
(25) Katritzky, A. R.; De Rosa, M.; Grzeskowiak, N. E. Pyrylium-mediated transformations of natural products. Part 1. Synthesis and hydrolysis of 4-(4- methoxy-3-sulphophenyl)-2,6-bis-(4-sulphophenyl)pyrylium perchlorate: a new water-soluble pyrylium cation. *J. Chem. Soc., Perkin Trans. 2* **1984**, 841−847.
(26) Katritzky, A. R.; Yang, Y.-K.; Gabrielsen, B.; Marquet, J. Pyrylium-mediated transformations of Natural Products. Part 3.[1] Synthesis of water-soluble pyrylium salts and their preparative reactions with amines. *J. Chem. Soc., Perkin Trans. 2* **1984**, 857−866.
(27) Katritzky, A. R.; Leahy, D. E. Pyrylium-mediated transformations of natural products. Part 4.[1] Reactions of water-soluble pyrylium salts with water and with amines. *J. Chem. Soc., Perkin Trans. 2* **1984**, 867−873.
(28) Teegarden, D. M.; Herkstroeter, W. G.; McColgin, W. C. Contrast enhancement lithography system based on pyrylium dye bleach chemistry. *J. Imaging Sci. Technol.* **1993**, *37*, 149−155.
(29) Ye, J.; Zhang, X.; Deng, D.; Ning, G.; Liu, T.; Zhuang, M.; Yang, L.; Gong, W.; Lin, Y. Selective C−C bond cleavage of cyclopentadiene rings assisted by ferric chloride to synthesize water-soluble pyrylium salts. *RSC Adv.* **2013**, *3*, 8232−8235.
(30) Montes-Navajas, P.; Teruel, L.; Corma, A.; Garcia, H. Specific binding effects for cucurbit[8]uril in 2,4,6-triphenylpyrylium−cucurbit[8]uril host−guest complexes: observation of room-temperature phosphorescence and their application in electroluminescence. *Chem. − Eur. J.* **2008**, *14*, 1762−1768.
(31) Fakis, M.; Tsigaridas, G.; Polyzos, I.; Giannetas, V.; Persephonis, P.; Spiliopoulos, I.; Mikroyannidis, J. Intensity dependent nonlinear absorption of pyrylium chromophores. *Chem. Phys. Lett.* **2001**, *342*, 155−161.
(32) Polyzos, I.; Tsigaridas, G.; Fakis, M.; Giannetas, V.; Persephonis, P.; Mikroyannidis, J. Two-photon absorption properties of novel organic materials for three-dimensional optical memories. *Chem. Phys. Lett.* **2003**, *369*, 264−268.
(33) Jha, P. C.; Luo, Y.; Polyzos, I.; Persephonis, P.; Ågren, H. Two- and three-photon absorption of organic ionic pyrylium based materials. *J. Chem. Phys.* **2009**, *130*, No. 174312.
(34) Holtgrewe, N.; Greenberg, E.; Prescher, C.; Prakapenka, V. B.; Goncharov, A. F. Advanced integrated optical spectroscopy system for diamond anvil cell studies at GSECARS. *High Press. Res.* **2019**, *39*, 457−470.
(35) Chadwick, T. C. 2,4,6-Triphenylpyrylium chloride. A new organic analytical reagent for the determination of certain anions. *Anal. Chem.* **1973**, *45*, 985−986.
(36) Sitze, M. S.; Schreiter, E. R.; Patterson, E. V.; Freeman, R. G. Ionic liquids based on $FeCl_3$ and $FeCl_2$. Raman scattering and ab Initio calculations. *Inorg. Chem.* **2001**, *40*, 2298−2304.
(37) Balaban, A. T. Aromaticity of Six-Membered Rings with One Heteroatom. In *Aromaticity in Heterocyclic Compounds*; Krygowski, T. M.; Cyranski, M. K., Eds.; Topics in Heterocyclic Chemistry; Springer-Verlag: Berlin, 2009; Vol. *19*, pp 203−246.
(38) Katritzky, A. R.; Horvath, K.; Plau, B. The conversion of primary aliphatic amines into chlorides by reaction with 2,4,6-triphenylpyrylium chloride. *Synthesis* **1979**, *1979*, 437−438.
(39) Balaban, A. T.; Dinculescu, A.; Orofino, G. N.; Fischer, G. W.; Koblik, A. V.; Mezheritskii, V. V.; Schroth, W. *Advances in Heterocyclic Chemistry*; Katritzky, A. R., Ed.; Academic: New York, 1982; Vol. *2*, p 1.
(40) Haucke, G.; Czerney, P.; Cebulla, F. Absorption and fluorescence of pyrylium salts. *Ber. Bunsenges. Phys. Chem.* **1992**, *96*, 880−886.
(41) Resta, I. M.; Lucantoni, F.; Apostolova, N.; Galindo, F. Fluorescent styrylpyrylium probes for the imaging of mitochondria in live cells. *Org. Biomol. Chem.* **2021**, *19*, 9043−9057.
(42) Wen, S.-Y.; Zhang, W.; Ren, T.-B.; Zhang, Q.-L.; Liu, Y.-P.; Shi, L.; Hu, R.; Zhang, X.-B.; Yuan, L. Donor and ring-fusing engineering for far-red to near-infrared triphenylpyrylium fluorophores with enhanced fluorescence performance for sensing and imaging. *Chem. − Eur. J.* **2019**, *25*, 6973−6979.
(43) Onishi, S.; Suzuki, Y.; Ano, H.; Kawamata, J. Water-soluble red-fluorescent dyes for two- photon deep-tissue imaging. *Bull. Chem. Soc. Jpn.* **2020**, *93*, 1226−1233.
(44) Xu, C.; Webb, W. W. Measurement of two-photon excitation cross sections of molecular fluorophores with data from 690 to 1050 nm. *J. Opt. Soc. Am. B* **1996**, *13*, 481−491.
(45) Nag, A.; Goswami, D. Solvent effect on two-photon absorption and fluorescence of rhodamine dyes. *J. Photochem. Photobiol. A* **2009**, *206*, 188−197.
(46) Makarov, N. S.; Drobizhev, M.; Rebane, A. Two-photon absorption standards in the 550−1600 nm excitation wavelength range. *Opt. Express* **2008**, *16*, 4029−4047.
(47) Magut, P. K. S.; Das, S.; Fernand, V. E.; Losso, J.; McDonough, K.; Naylor, B. M.; Aggarwal, S.; Warner, I. M. Tunable cytotoxicity of Rhodamine 6G via anion variations. *J. Am. Chem. Soc.* **2013**, *135*, 15873−15879.
(48) Broadwater, D.; Bates, M.; Jayaram, M.; Young, M.; He, J.; Raithel, A. L.; Hamann, T. W.; Zhang, W.; Borhan, B.; Lunt, R. R.; Lunt, S. Y. Modulating cellular cytotoxicity and phototoxicity of fuorescent organic salts through counterion pairing. *Sci. Rep.* **2019**, *9*, No. 15288.
(49) Denk, W.; Strickler, J. H.; Webb, W. W. Two-photon laser scanning fluorescence microscopy. *Science* **1990**, *248*, 73−76.
(50) Canasa, P.; King, D.; Cifligu, P.; Lua Sanchez, A. F.; Chen, S. L.; Han, H.; T Malik, T.; Billinghurst, B.; Zhao, J.; Park, C.; Rossman, G. R.; Pravica, M.; Bhowmik, P. K.; Evlyukhin, E. Piezochromic behavior of 2,4,6-triphenylpyrylium tetrachloroferrate. *Small Sci.* **2024**, *4*, No. 2400106.

https://doi.org/10.1021/acs.jpcb.4c03934
J. Phys. Chem. B 2024, 128, 9815−9828

(51) Descalzo, A. B.; Martínez-Máñez, R.; Sancenón, F.; Hoffmann, K.; Rurack, K. The supramolecular chemistry of organic−inorganic hybrid materials. *Angew. Chem., Int. Ed.* **2006**, *45*, 5924−5948.
(52) Evlyukhin, E.; Museur, L.; Diaz-Gomez-Trevino, A. P.; Traore, M.; Brinza, O.; A Zerr, A.; Kanaev, A. Synthesis of organic−inorganic hybrids via a high pressure-ramp process: the effect of inorganic nanoparticle loading on structural and photochromic properties. *Nanoscale* **2018**, *10*, 22293−22301.
(53) Martínez-Máñez, R.; Sancenón, F. Chemodosimeters and 3D inorganic functionalised hosts for the fluoro-chromogenic sensing of anions. *Coord. Chem. Rev.* **2006**, *250*, 3081−3093.

https://doi.org/10.1021/acs.jpcb.4c03934
J. Phys. Chem. B 2024, 128, 9815−9828